

## Location of Moderate-Sized Earthquakes Recorded by the NARS–Baja Array in the Gulf of California Region Between 2002 and 2006

RAUL R. CASTRO,<sup>1</sup> ARTURO PEREZ-VERTTI,<sup>1</sup> IGNACIO MENDEZ,<sup>1</sup> ANTONIO MENDOZA,<sup>1</sup> and LUIS INZUNZA<sup>1</sup>

**Abstract**—We relocated the hypocentral coordinates of small to moderate-sized earthquakes reported by the National Earthquake Information Center (NEIC) between April 2002 and August 2006 in the Gulf of California region and recorded by the broadband stations of the network of autonomously recording seismographs (NARS–Baja array). The NARS–Baja array consists of 19 stations installed in the Baja California peninsula, Sonora and Sinaloa, Mexico. The events reported by the preliminary determinations of epicenters (PDE) catalog within the period of interest have moment magnitudes ( $M_w$ ) ranging between 1.1 and 6.7. We estimated the hypocentral location of these events using  $P$  and  $S$  wave arrivals recorded by the regional broadband stations of the NARS–Baja and the RESBAN (*Red Sismológica de Banda Ancha*) arrays and using a standard location procedure with the HYPOCENTER code (LIENERT and HAVSKOV in *Seism Res Lett* 66:26–36, 1995) as a preliminary step. To refine the location of the initial hypocenters, we used the shrinking box source-specific station term method of LIN and SHEARER (*J Geophys Res* 110, B04304, 2005). We found that most of the seismicity is distributed in the NW–SE direction along the axis of the Gulf of California, following a linear trend that, from north to south, steps southward near the main basins (Wagner, Delfin, Guaymas, Carmen, Farallon, Pescadero and Alarcon) and spreading centers. We compared the epicentral locations reported in the PDE with the locations obtained using regional arrival times, and we found that earthquakes with magnitudes in the range 3.2–5.0  $mb$  differ on the average by as much as 43 km. For the  $M_w$  magnitude range between 5 and 6.7 the discrepancy is less, differing on the average by about 25 km. We found that the relocated epicenters correlate well with the main bathymetric features of the Gulf.

**Key words:** Seismicity, Gulf of California, Mexico.

### 1. Introduction

The transform faults and spreading centers of the Gulf of California (GoC hereafter) form a transform-rift plate boundary between the Pacific and the North American plates. The seismicity in this region consists of right lateral strike-slip events located near transform faults and normal fault earthquakes that occur mostly on the spreading centers (GOFF *et al.*, 1987). In the northern GoC, there are three active basins, from north to south: the Consag and Wagner basins; the upper Delfin basin; and the lower Delfin and Salsipuedes basins (Fig. 1). These basins are all distributed within a shallow depression. The lower Delfin basin has a high fault density and is magmatically the most active of the three (PERSAUD *et al.*, 2003). In general, the northern GoC has a more complex fault system than the southern GoC, where transform fault-spreading center geometry is dominant. The crust in the southern region of the Gulf is oceanic and thinner than in the northern GoC (ZHANG *et al.*, 2007) where the crust is not typically oceanic. In the southern GoC, the Guaymas basin seems to have a transitional crust, since it is different from the typical continental or oceanic crusts (EINSELE 1982; FABRIOL *et al.*, 1999). Farther south, the crust of the Alarcon basin is oceanic, based on magnetic anomaly lineations (DEMETS, 1995).

The GoC is characterized for having fast spreading centers (REICHLE and REID, 1977). Although earthquakes are not commonly observed from fast spreading centers (ISACKS *et al.*, 1968), these types of boundaries are seismically active in the GoC (REICHLE and REID, 1977). Previous studies of seismicity in this region have been done based on worldwide networks (e.g. SYKES, 1968, 1970; MOLNAR, 1973; GOFF *et al.*,

<sup>1</sup> División Ciencias de la Tierra, Departamento de Sismología, Centro de Investigación Científica y de Educación Superior de Ensenada (CICESE), Apartado Postal 2732, 22860 Ensenada, Baja California, Mexico. E-mail: raul@cicese.mx

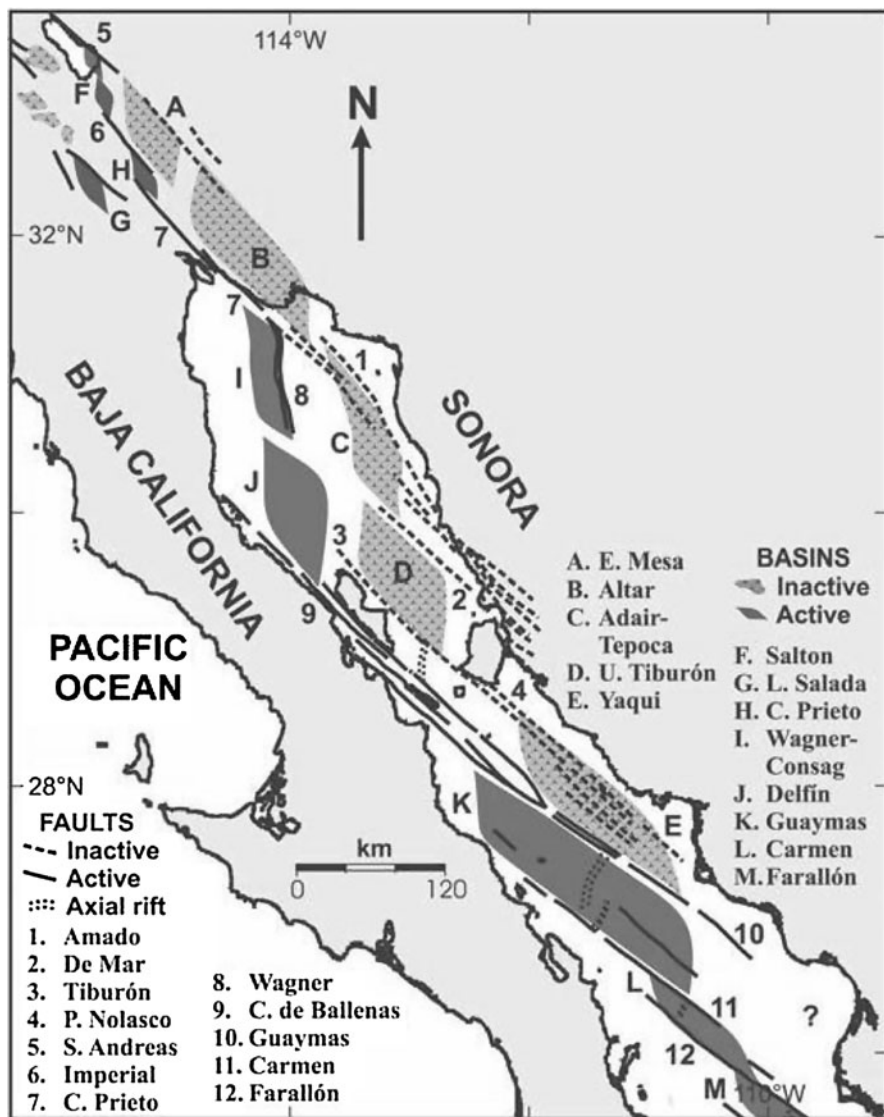


Figure 1  
Tectonic map of the region, modified from Aragón-Arreola and Martin-Barajas (2007)

1987) and a few using regional stations (LOMNITZ *et al.*, 1970) and sonobuoys data (THATCHER and BRUNE, 1971; REID *et al.*, 1973; REICHLE and REID, 1977).

In this paper, we present accurate located epicenters, from moderate magnitude earthquakes, obtained using regional data and modern location techniques. We will show that the epicentral distribution of the earthquakes analyzed correlates well with the main bathymetric features of the GoC region. We also evaluate the epicentral location

deviations expected from the preliminary determinations of epicenters (PDE) catalog.

## 2. Data

We picked arrival times from earthquakes reported by the PDE from April 2002 to August 2006 and recorded by the broadband stations of the NARS-Baja array (Network of Autonomously Recording Seismographs) (TRAMPERT *et al.*, 2003; CLAYTON

*et al.*, 2004) and the RESBAN array (Red Sismológica de Banda Ancha). The NARS–Baja array operated from the spring of 2002 to the fall of 2008 and consisted of 14 broadband seismic stations, provided by Utrecht University, with STS2 sensors, a global positioning system (GPS) and a 24-bit data logger. The RESBAN array started operating in 1995 with two broadband stations, one in Bahía de los Angeles, Baja California, and the other in Guaymas, Sonora (REBOLLAR *et al.*, 2001). During the period 2002–2006 three additional stations were added to the network. This array is operated by CICESE (Centro de Investigación Científica y de Educación Superior de Ensenada). The stations of RESBAN consist of Guralp CMG-40T or CMG-3ESP sensors, 24-bit

Guralp digitizers, a CMG-SAM2 acquisition module and GPS for time control. The stations of both arrays record continuously at 20 samples per second. The triangles in Fig. 2 show the distribution of the seismic stations of these arrays. Stations NE70–NE83 belong to the NARS–Baja array and the rest to RESBAN.

The data set consists of *P* and *S* wave arrival times handpicked, with an approximate accuracy of one tenth of a second, from the recordings of both broadband arrays from earthquakes that occurred between April 2002 and August 2006 and reported by PDE. The earthquakes analyzed range in  $M_w$  magnitude between 1.1 and 6.7, and are located between 22°N–31°N and 108°W–117°W.

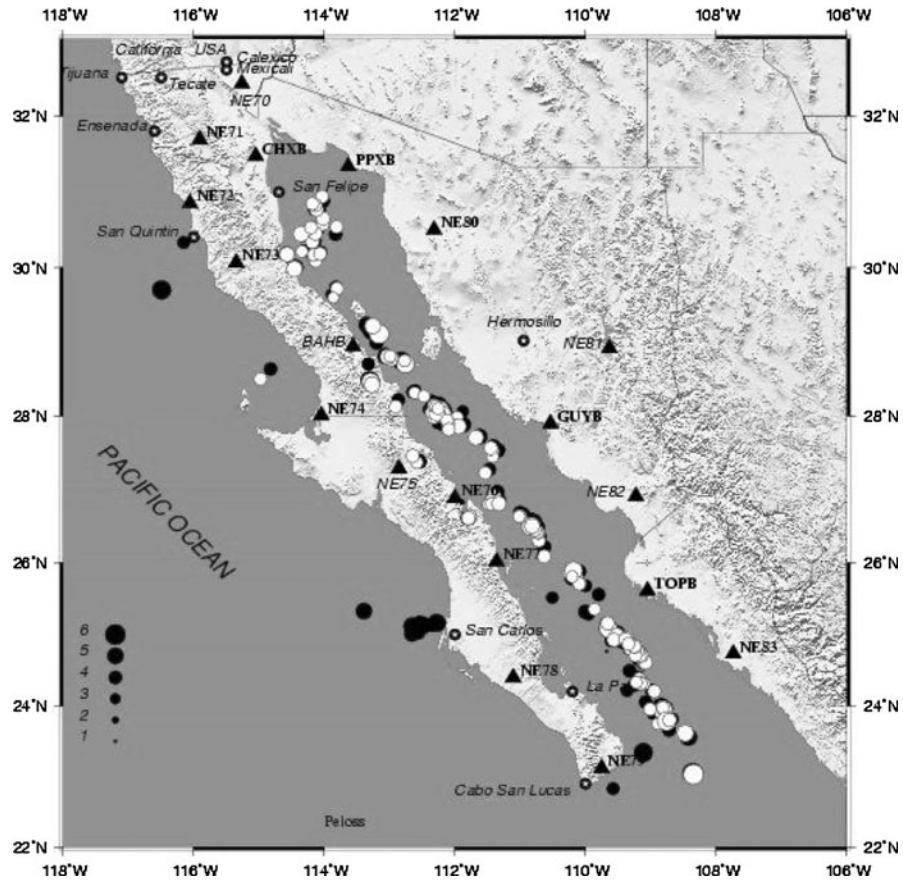


Figure 2

Earthquake epicenter location map. The black dots are epicenters reported by NEIC and relocated using arrival times of the broadband stations (triangles) of the NARS–Baja (NE70–NE83) and RESBAN (EXCB, BAHB, PPXB, GUAY, TOPB) arrays, and the HYPOCENTER code of LIENERT and HAVSKOV (1995). The white dots are the epicenters of the same data set but relocated using the SSST method of LIN and SHEARER (2005). The size of the circles is proportional to the magnitude of the earthquakes

### 3. Method

We calculated an initial hypocentral location with the HYPOCENTER code of LIENERT and HAVSKOV (1995) using at least four  $P$  and  $S$  wave arrival times from the stations shown in Fig. 2. For events reported by PDE in the northern GoC, between  $30^{\circ}\text{N}$  and  $31.5^{\circ}\text{N}$ , we used the velocity model obtained by NAVA and BRUNE (1982). This model is based on an approximate reverse refraction line obtained using a blast from Corona, Southern California ( $\sim 33.8^{\circ}\text{N}$ ,  $117.5^{\circ}\text{W}$ ) and the well-located Pino Solo earthquake ( $5.1\text{M}_L$ ) of July 1975 ( $31.82^{\circ}\text{N}$ ,  $115.85^{\circ}\text{W}$ ). This model consists of three layers with  $P$  velocities of  $6.57\text{--}6.95$  km/s, an upper mantle velocity of 8.0 km/s and a crustal thickness of approximately 42 km. For earthquakes reported in the lower Delfin basin, between  $28^{\circ}\text{N}$  and  $30^{\circ}\text{N}$ , we used a velocity model based on surface wave analysis (LÓPEZ-PINEDA *et al.*, 2007). This model is composed by four horizontal layers with  $P$  velocities of  $4.6\text{--}7.9$  km/s, an upper mantle velocity of 8.2 km/s and a crustal thickness of 40 km. For events in the Guaymas basin and the southern end of the GoC, we used the velocity structure proposed by FABRIOL *et al.* (1999) for the Tortuga rift, on the western margin of the GoC. This velocity model consists of four homogenous layers with  $P$  wave velocities of  $4.0\text{--}6.9$  km/s over a half-space with a  $P$  velocity of 7.6 km/s and a crustal

thickness of 24 km. The comparison of these velocity models is shown in Fig. 3a. The black dots in Fig. 2 show the distribution of the epicenters located using these models and the body wave arrivals recorded in the regional stations of the NARS-Baja and the RESBAN arrays.

To account for lateral heterogeneities of the velocity structure the HYPOCENTER code uses static station terms (ST). The ST correction is determined by the mean of the travel-time residuals from all the events recorded at a given station. This approach is adequate if the source-station paths are the same for all the events. However, in the GoC the seismicity is distributed over a large region (Fig. 2) and the ST do not account completely for the travel-time perturbation introduced by lateral velocity heterogeneities. The use of source-specific station terms (SSST) as proposed by RICHARDS-DINGER and SHEARER (2000), is a better technique, since each station has a correction function that varies with source position. A generalization of the SSST method was implemented by LIN and SHEARER (2005) in their COMPLOC earthquake location code. We used a modified version of the COMPLOC code that permits the use of regional phases ( $Pn$ ,  $Pg$ ,  $Sn$ ,  $Sg$ ) and weights the phase arrival picks according to the source-station distance (e.g. CASTRO *et al.*, 2010).

To minimize regional variations of the velocity structure, we relocated the hypocenters dividing the

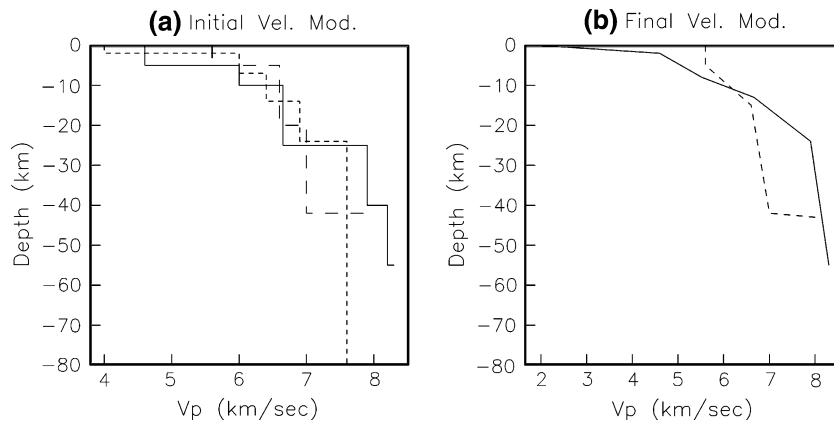


Figure 3

$P$  wave velocity models tested. **a** Initial models used to locate the events with HYPOCENTER. Solid lines correspond to the model of LOPEZ-PINEDA *et al.* (2007), dashed lines to the model of NAVA and BRUNE (1982) and dotted lines to the model of FABRIOL *et al.* (1999). **b** Additional models tested. Dashed line is a model based on NAVA and BRUNE'S (1982) but with vertical gradients. The model obtained by GONZALEZ-FERNANDEZ *et al.* (2005) is represented with solid lines

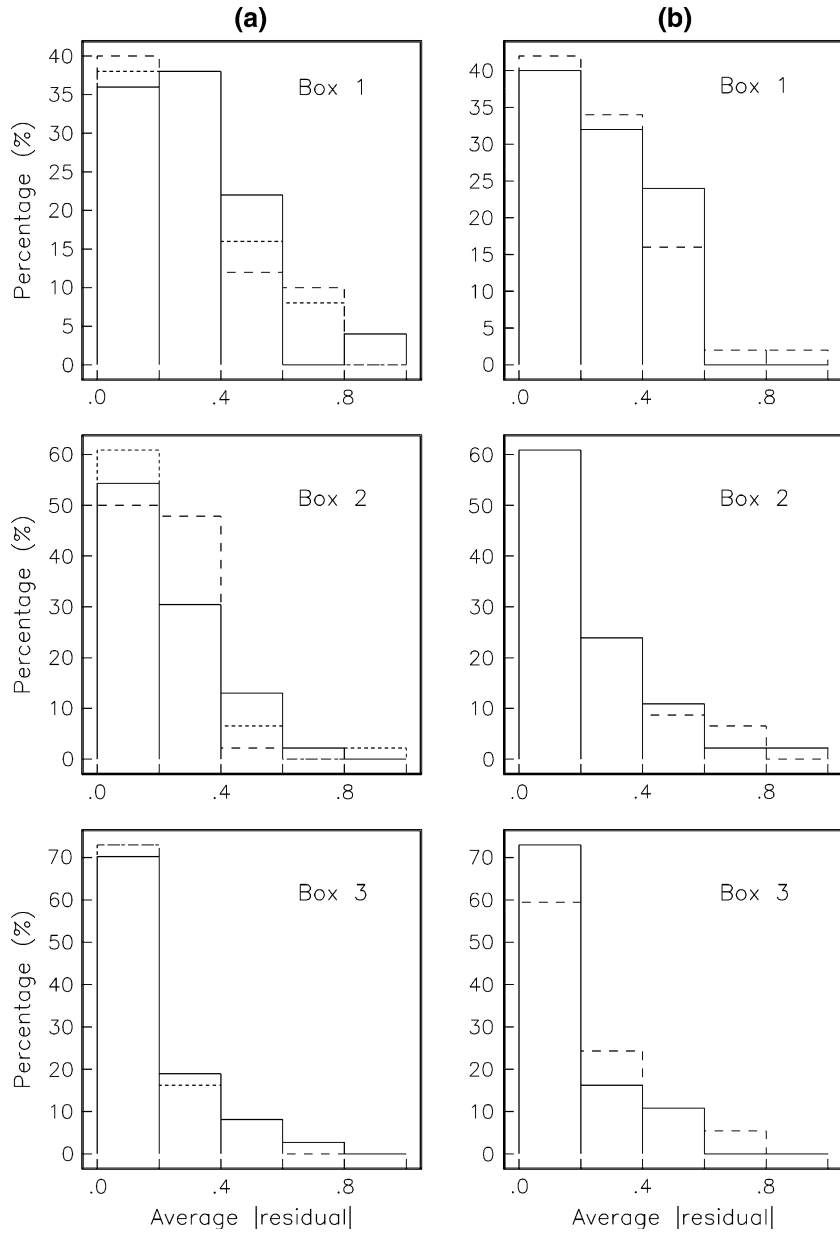


Figure 4

Average of the absolute value of the travel time residuals obtained using different velocity models. Column *a* shows histograms of residuals for the three rectangles used to divide the GoC region. Solid lines were used to represent residuals obtained with the velocity model of LOPEZ-PINEDA *et al.* (2007), dashed lines correspond to residuals obtained with the model proposed by NAVA and BRUNE (1982) and for the velocity model obtained by FABRIOL *et al.* (1999) we used dotted lines. Column *b* shows with dashed lines the residuals obtained using a model similar to that of NAVA and BRUNE (1982) but with vertical gradients. The solid lines correspond to the residuals obtained with the model of GONZALEZ-FERNANDEZ *et al.* (2005)

GoC region into three rectangles based on the distribution of the epicenters located with HYPOCENTER (Fig. 2). One of the rectangles covered from the San Pedro Martir basin ( $28^{\circ}\text{N}$ ) to the Wagner basin

( $31.5^{\circ}\text{N}$ ), another from Farallon basin ( $25.5^{\circ}\text{N}$ ) to the northern Guaymas basin ( $28^{\circ}\text{N}$ ) and the last one from the southern end of the GoC ( $22^{\circ}\text{N}$ ) to the Farallon basin. We relocated the hypocenters using records

from all the stations available regardless of the rectangle but only the events within the corresponding rectangle were used to calculate the SSST. We tested the three velocity models described above (Fig. 3a) and two additional models (Fig. 3b) to relocate the earthquakes in each rectangle. One of these models, represented with dashed lines in Fig. 3b, is similar to that proposed by NAVA and BRUNE (1982), but we introduced vertical velocity gradients. The other velocity model (solid line in Fig. 3b) was proposed by GONZALEZ-FERNANDEZ *et al.* (2005) for the northern GoC and is based on a 280-km-long profile that included deep multi-channel seismic reflection data, densely sampled refraction data and wide-angle reflection information. This model is consistent with that obtained by PHILLIPS (1964) using active sources and sonobouys. The model of GONZALEZ-FERNANDEZ *et al.* (2005) consists of four layers. The first layer represents the uppermost sediments, and it has  $P$  wave velocities between 1.77 and 2.15 km/s. The second layer, corresponding to lower sediments, has velocities between 4.11 and 5.09 km/s. The middle crust is represented by a layer with velocities of 5.37–5.67 km/s. The lower crust has velocities of 6.58–6.73 km/s, and below the Moho (at 24–25 km depth) is the upper mantle with a velocity of 7.9 km/s.

We calculated average travel time residuals using the five velocity models tested. Column a of Fig. 4 shows histograms calculated every 0.2 s for each of the rectangles, from north to south, used to divide the GoC region. This column shows the average residuals obtained with the SSST method and the three initial velocity models used to locate the earthquakes. For the northern GoC (Box 1) the model of NAVA and BRUNE (1982) gives the smaller average residuals and for the southern GoC (Box 3) the model of LOPEZ-PINEDA *et al.* (2007). In general, the velocity models that have a vertical velocity gradient (column b in Fig. 4) give the smaller residuals, particularly the model of GONZALEZ-FERNANDEZ *et al.* (2005), shown with solid lines in Fig. 4b.

#### 4. Results

We used the velocity model obtained by GONZALEZ-FERNANDEZ *et al.* (2005) for the final

estimates of the hypocentral coordinates. Figure 5 shows the histogram of focal depths obtained with the final locations. Most earthquakes have focal depths of less than 10 km and 52% have depths of less than 5 km. The lower maps of Figs. 6, 7, 8 and 9 show the final distribution of epicenters for different regions of the GoC and Fig. 10 shows the global distribution of the bigger earthquakes ( $M_w$  4.8–6.6). We also compared in Fig. 2 the initial locations obtained with HYPOCENTER (black dots) and the relocated epicenters using the SSST method (white dots). In many cases the epicentral locations obtained with these two methods are not very different because, as described above, when we located the epicenters with the HYPOCENTER code we used different velocity models depending on the initial location reported by PDE and according with the region. By doing this the static station corrections calculated with HYPOCENTER became space dependent. When we relocated the hypocenters using the SSST method, we used the same velocity model for all regions but we calculated specific stations terms that depend on the spatial distribution of the events surrounding the target event. In contrast, the epicenters reported in the PDE catalog show important differences with respect to the relocated epicenters using the SSST method (Fig. 11).

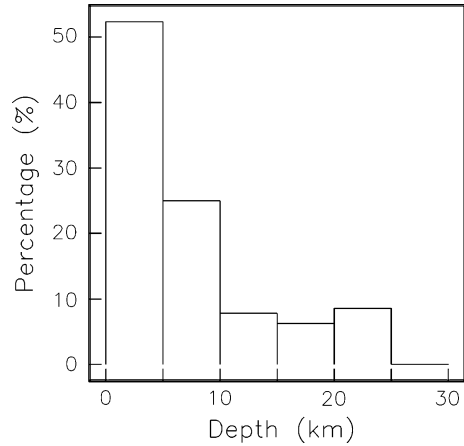


Figure 5  
Histogram of focal depths of the relocated hypocenters (using regional arrival times, the SSST method and the velocity model of GONZALEZ-FERNANDEZ *et al.*, 2005)

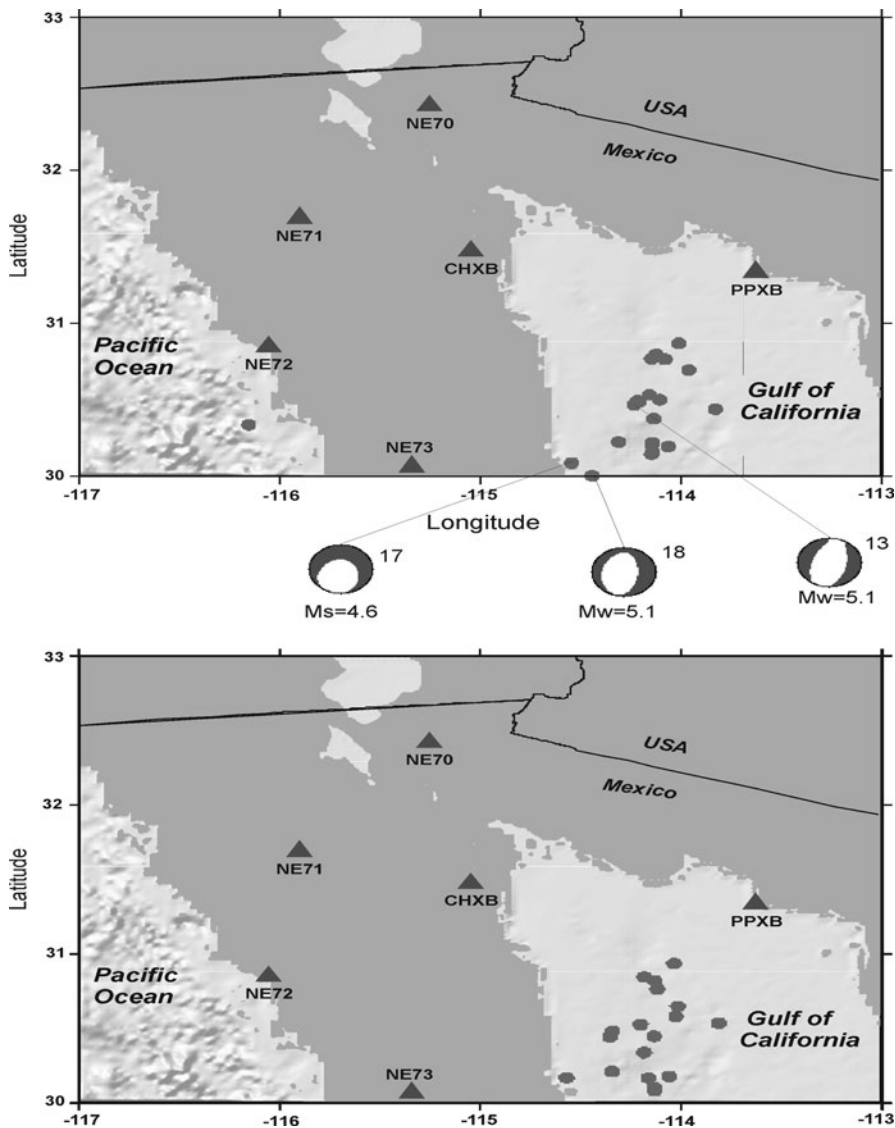


Figure 6

*Upper map* shows epicenters located with HYPOCENTER and the focal mechanisms available in the Harvard CMT catalog. The *lower map* shows the epicentral locations obtained using the SSST method of LIN and SHEARER (2005)

Comparing the epicentral locations reported by PDE with the relocated epicentral coordinates obtained with the regional arrival times and the SSST method (Fig. 11), we found that earthquakes with  $mb$  magnitudes in the range 3.2–5.0 differ on the average by as much as 43 km. For earthquakes with  $M_w$  magnitude between 5.0 and 6.7 the discrepancy is less, differing on the average by about 25 km. In general, the epicenters reported by PDE are shifted towards the northeast, where most seismic stations in North America are located.

#### 4.1. The Consag, Wagner and Upper Delfin Basins

On the northern end of this region ( $30.0^{\circ}\text{N}$ – $31.0^{\circ}\text{N}$ ) the epicenters are disperse in the middle of the GoC (Fig. 6). However, the most northern events ( $30.4^{\circ}\text{N}$ – $31.0^{\circ}\text{N}$ ) tend to align in the NW–SE direction. This part of the Gulf is characterized for having a complex fault system where multiple oblique-slip faults interact with each other (PERSAUD *et al.*, 2003). South of  $30.5^{\circ}\text{N}$  the earthquakes scatter toward the western margin of the GoC and for the period

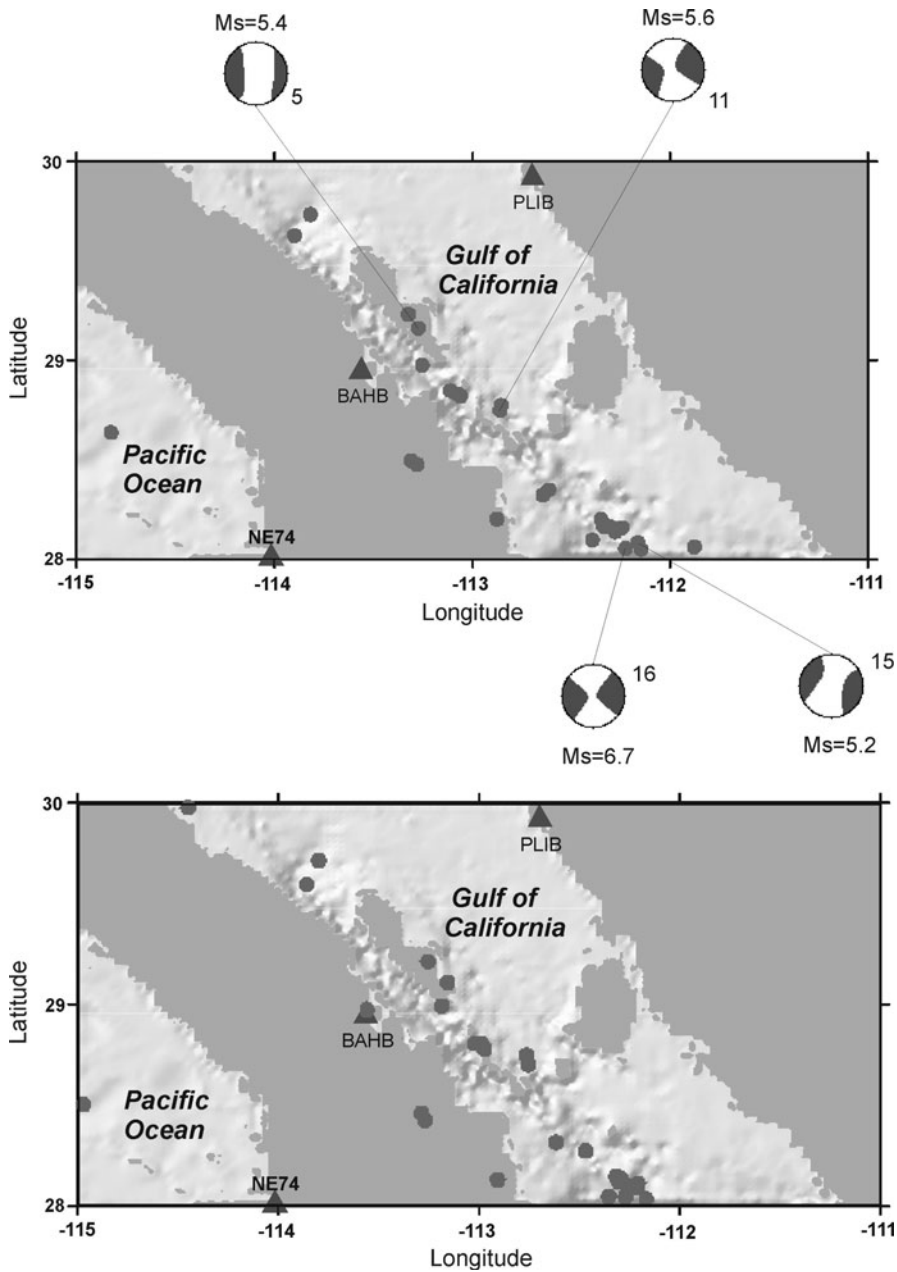


Figure 7  
Same as in Fig. 6 but for the San Pedro Martir–Delfin basins

analyzed the bigger events have normal fault mechanisms (upper map of Fig. 6).

#### 4.2. The Lower Delfin Basin and Canal de Ballenas

We relocated two events in the lower Delfin basin, distributed in the NE–SW direction, approximately

perpendicular to the GoC axis. However, most events align near the Canal de Ballenas fault, which is located between the station BAHB and the Angel de la Guarda island (Fig. 7). This transform fault is oriented in the NW–SE direction and runs from the northern end of Angel de la Guarda ( $\sim 29.5^\circ\text{N}$ ) to the south, where most of the epicenters are located

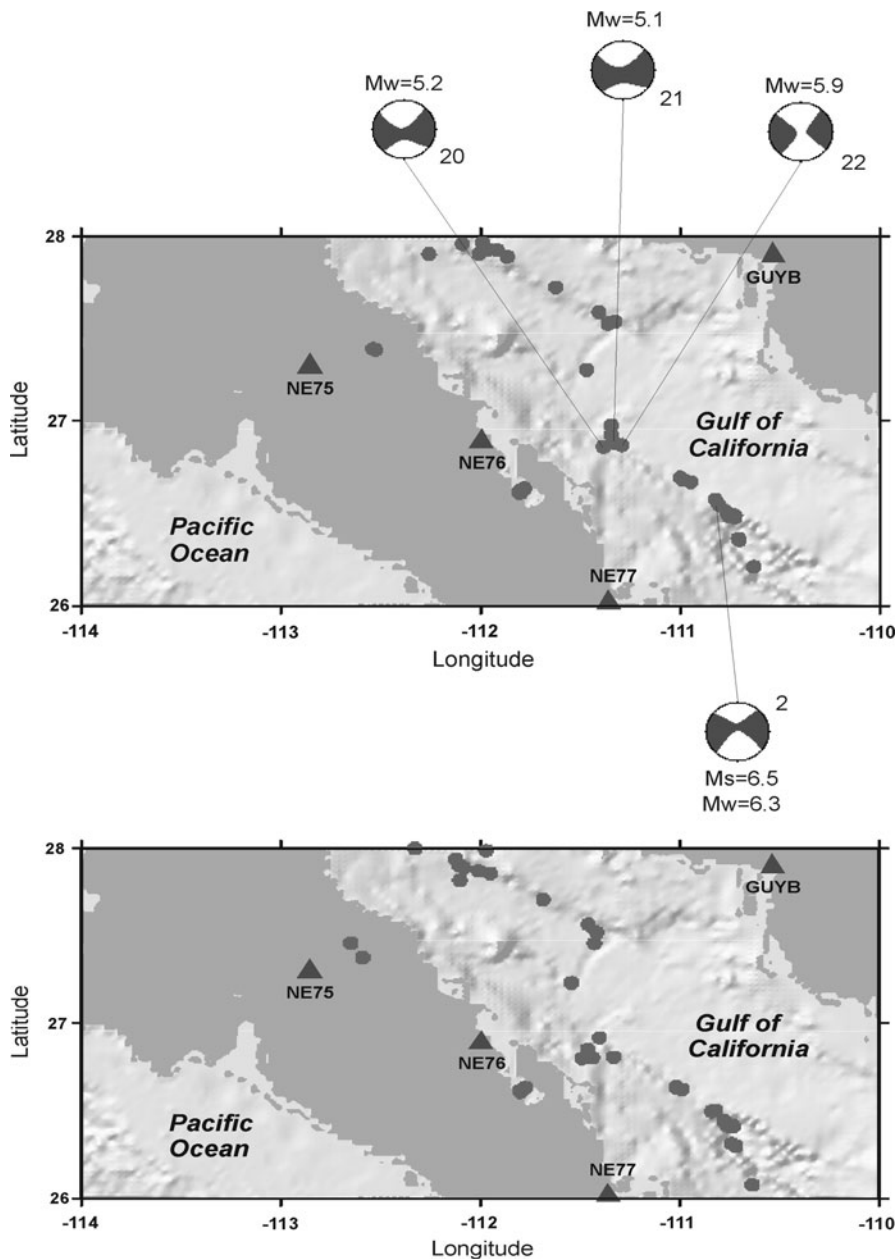


Figure 8  
Same as in Fig. 6 but for the Carmen–Guaymas basins

( $\sim 28.1^\circ\text{N}$ ). In this region the events have strike-slip focal mechanisms (upper map of Fig. 7). RODRIGUEZ-LOZOYA *et al.* (2008) studied events 5 and 11 (see Table 1 and upper map of Fig. 7). The earthquake located near the island Angel de la Guarda (event 5) occurred on November 12, 2003, they estimated a  $M_w = 5.6$  and a focal mechanism solution

corresponding to a normal fault striking  $301^\circ$ . Event 11 occurred on 24 September 2004 northwest of island San Lorenzo. RODRIGUEZ-LOZOYA *et al.* (2008) estimated an  $M_w = 5.8$  and a right-lateral strike-slip fault mechanism (strike =  $117^\circ$ , dip =  $75^\circ$ , rake =  $175^\circ$ ). Notice also in Fig. 7 that a few smaller events were located in the stable, central part of the Baja Peninsula

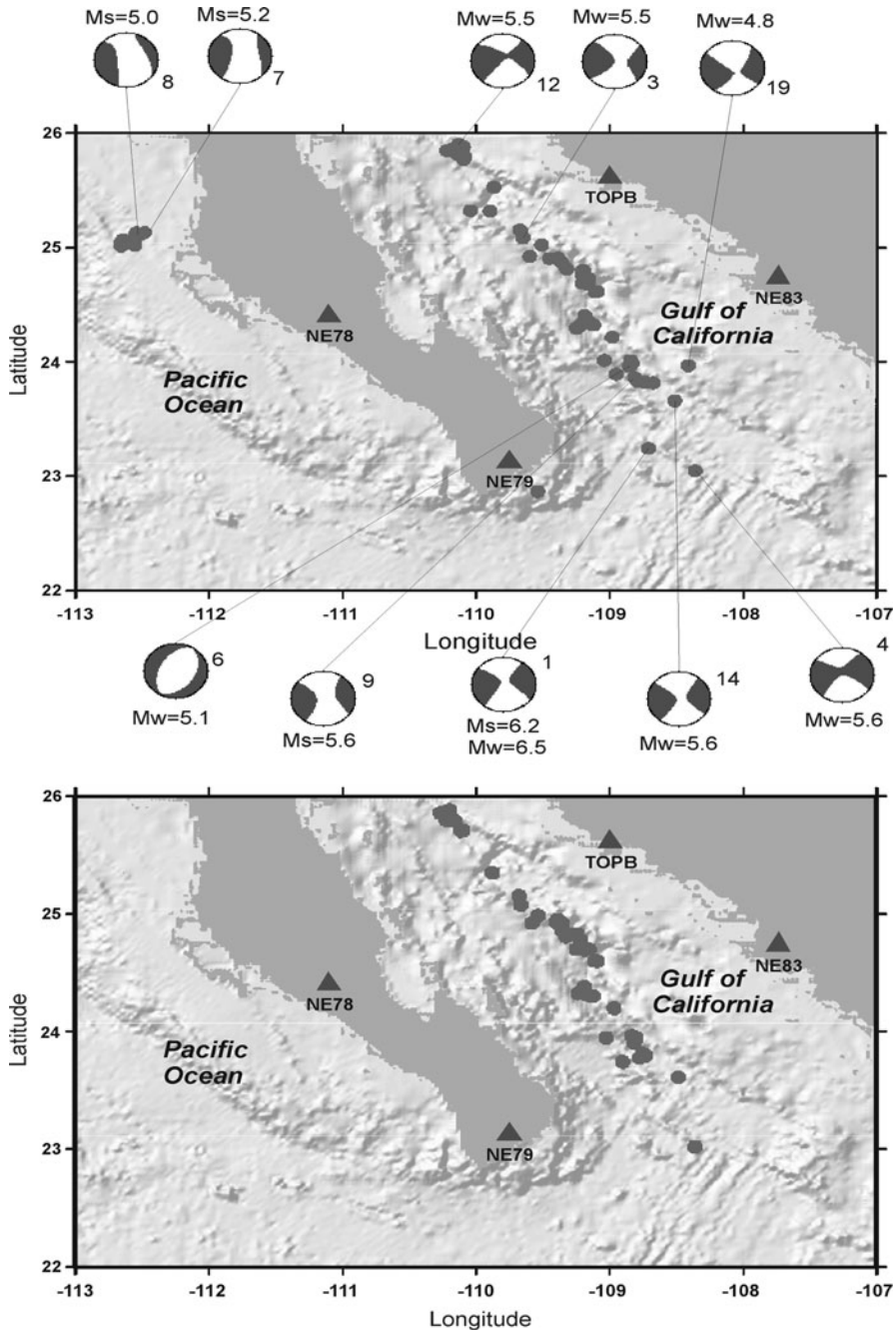


Figure 9  
Same as in Fig. 6 but from the southern end of the Gulf of California to the Farallon basins

where the unextended and relatively unfaulted crust is not expected to have seismic activity. Thus, these events may result as the response of the Pacific plate to the stress accumulated due to extensional forces from the GoC.

#### 4.3. Guaymas and Carmen Basins

This is a region of the GoC where some of the bigger events have occurred, particularly on the transform faults that connect the Guaymas and Carmen basins (Fig. 1). The earthquake of 12 March

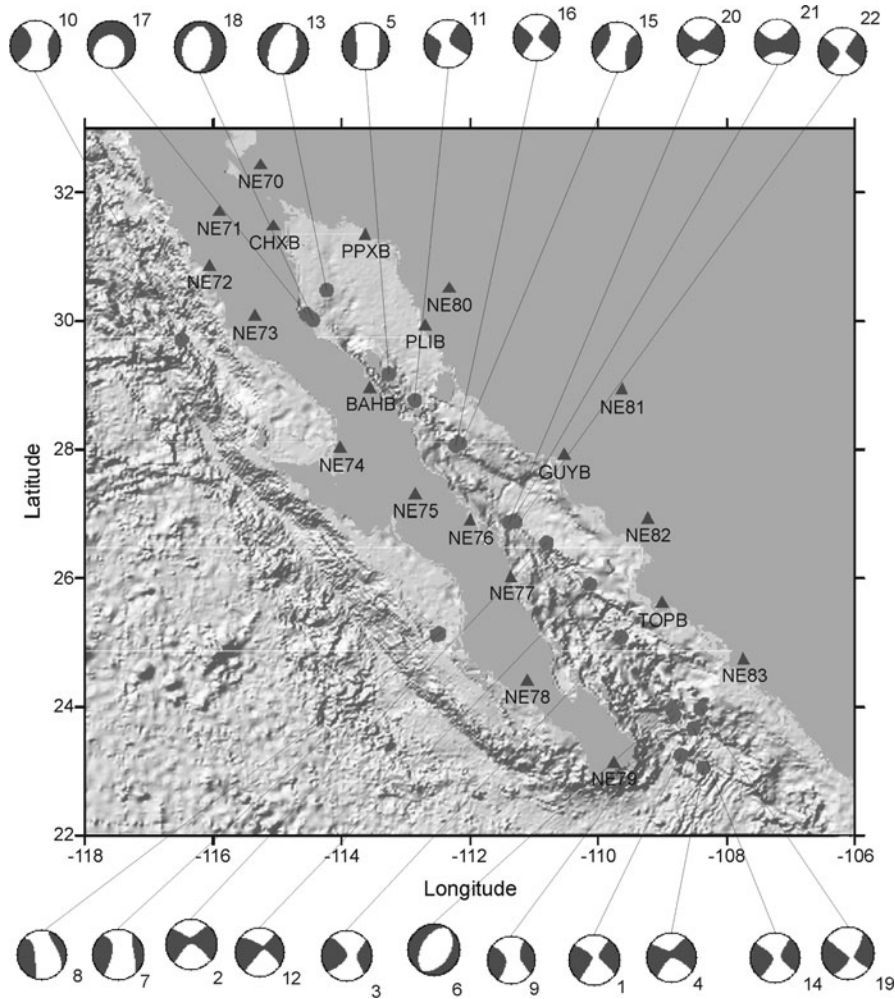


Figure 10  
Distribution of main events ( $M_w$  4.8–6.6) and focal mechanisms taken from the Global CMT Catalog

2003,  $M_w = 6.3$  (event 2 in Table 1 and upper map of Fig. 8) and a foreshock of  $M_w = 4.2$  were studied by LÓPEZ-PINEDA and REBOLLAR (2005). They calculated an  $M_w = 6.2$  and a focal mechanism consistent with a right-lateral strike-slip event (strike =  $117^\circ$ , dip =  $79^\circ$ , rake =  $168^\circ$ ). Other important events in this region have occurred in 1971 ( $M_w = 6.5$ ), 1974 ( $M_w = 6.3$ ), 1988 ( $M_w = 6.6$ ) and 1995 ( $M_w = 6.0$ ) (LÓPEZ-PINEDA and REBOLLAR 2005). South of Carmen basin ( $26^\circ\text{N}$ ,  $110^\circ\text{W}$ ) PACHECO and SYKES (1992) also reported an earthquake with  $M_w = 7.0$  that occurred on 07 January 1901. The relocated epicenters for the 2002–2006 interval (lower map of Fig. 8) tend to align in the NW–SE direction between  $27.6^\circ\text{N}$  and

$28^\circ\text{N}$ , where the transform fault that connects the San Pedro Martir basin with the Guaymas basin can be inferred from the bathymetry (LONSDALE 1989). Farther south ( $\sim 27^\circ\text{N}$ ), in the Guaymas basin, the seismicity jumps towards the western margin of the Gulf and aligns again in the NW–SE direction along the transform fault that connects the Guaymas and Carmen basins.

#### 4.4. Farallon, Pescadero and Alarcon Basins

This region is the most active of the four. Figure 9 shows the distribution of the relocated epicenters and the focal mechanism reported by the Global CMT

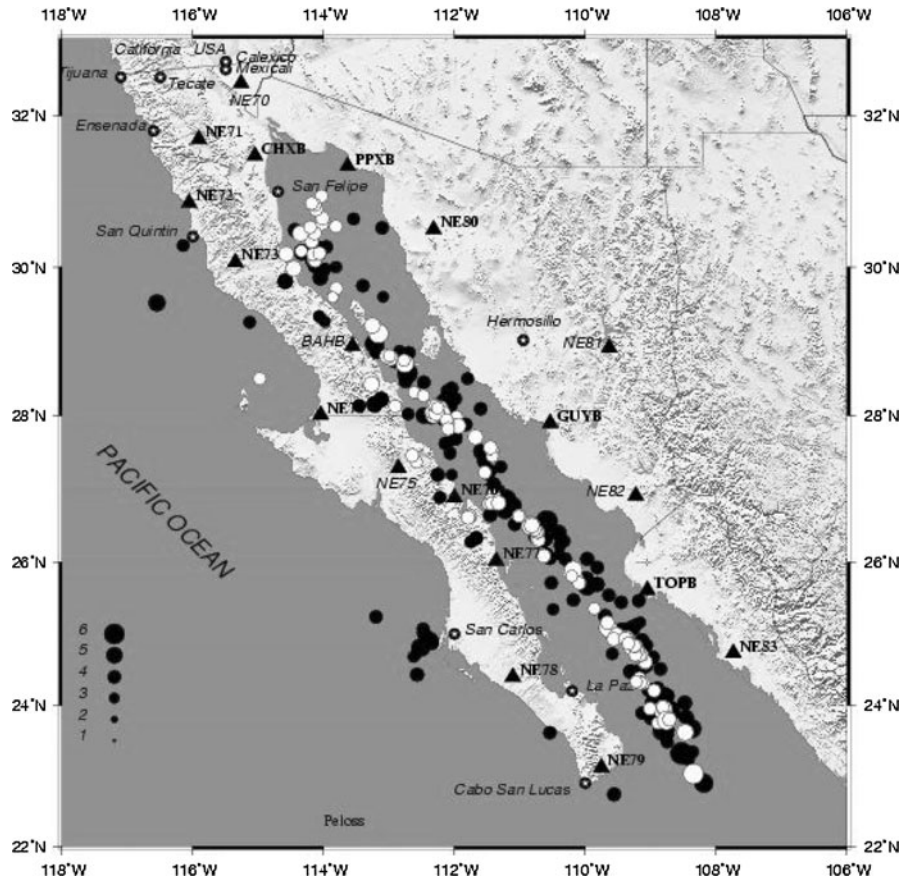


Figure 11

Earthquake epicenter location map. The black dots are epicenters reported by NEIC. White dots are the epicenters relocated using the SSST method of LIN and SHEARER (2005) and arrival times of the regional stations of NARS–Baja and RESBAN seismic networks. The size of the circles is proportional to the magnitude of the earthquakes

Catalog for the bigger events. Most of these earthquakes are strike-slip events, although normal fault events also occur in this region. Event 6 ( $M_w = 5.1$ ) of Table 1, upper map of Fig. 9, is a normal fault earthquake. Northwest of Farallon basin ( $\sim 25.9^\circ\text{N}$ ,  $110.1^\circ\text{W}$ ) we relocated a cluster of earthquakes, where on February 22, 2005 occurred event 12 ( $M_w = 5.5$ ). This cluster is located on the transform fault that connects the Carmen and Farallon basins. RODRIGUEZ-LOZOYA *et al.* (2008) calculated the focal mechanism of event 12 and found that the best solution is consistent with a right-lateral strike-slip fault (strike =  $309^\circ$ , dip =  $65^\circ$ , rake =  $159^\circ$ ). Note that southwest of the cluster, there are some events located on the spreading center, near the Farallon basin, that connects to another transform fault to the

south. This transform fault extends toward the southeast, where we relocated another group of earthquakes aligning in the NW–SE direction. Another group of earthquakes that jump towards the south, between  $108.5^\circ\text{W}$  and  $109^\circ\text{W}$ , are located on the transform fault that connects Pescadero and Alarcon basins.

Figure 10 summarizes the location and focal mechanisms of the main events relocated in the 2002–2006 period. Most of the events (68%) are strike-slip events associated to the transform faults of the GoC. Only seven events are normal fault earthquakes and have magnitudes  $M_w \leq 5.6$ , indicating that most of the seismic energy is relieved along the transform faults of the GoC, where the bigger strike-slip events occur.

Table 1

*Coordinates of events shown in Fig. 10, taken from the Global CMT catalog*

	Date	Time	Lat.	Lon.	H	$M_w$
1	2002-10-03	16:08:41	23.22	-108.27	15.0	6.5
2	2003-03-12	23:41:39	26.63	-110.91	15.0	6.3
3	2003-04-15	08:21:21	25.51	-109.60	15.0	5.5
4	2003-07-02	05:11:40	23.11	-108.33	15.0	5.6
5	2003-11-12	04:55:01	29.34	-113.45	15.0	5.6
6	2004-02-09	00:01:48	24.04	-108.93	12.0	5.1
7	2004-02-09	01:24:40	25.06	-112.60	12.0	5.4
8	2004-02-09	09:03:50	25.13	-112.56	12.0	5.3
9	2004-02-18	10:59:25	23.91	-108.75	12.6	5.8
10	2004-08-30	05:35:18	29.61	-116.59	12.0	5.1
11	2004-09-24	14:43:14	28.82	-112.99	12.0	5.9
12	2005-02-22	19:15:52	25.82	-110.09	18.9	5.5
13	2005-04-27	00:32:60	30.45	-114.27	12.0	5.1
14	2005-06-05	08:28:52	23.70	-108.51	12.0	5.6
15	2006-01-04	01:05:12	28.32	-112.28	12.0	5.2
16	2006-01-04	08:32:37	28.38	-112.51	15.0	6.6
17	2006-05-01	20:53:22	30.41	-114.46	13.8	4.9
18	2006-05-01	21:04:41	30.13	-114.49	12.0	5.1
19	2006-05-11	11:02:52	24.16	-108.83	12.0	4.8
20	2006-05-28	14:02:59	26.96	-111.34	19.1	5.2
21	2006-05-28	14:18:08	27.00	-111.32	17.3	5.1
22	2006-07-30	01:21:01	26.87	-111.36	22.9	5.9

### 5. Conclusions

We relocated 128 hypocenters of earthquakes with  $M_w$  magnitudes 1.1–6.7 reported by PDE between April 2002 and August 2006 using regional arrival times recorded by the NARS–Baja and RESBAN arrays. We found that earthquakes with magnitudes in the range 3.2–5.0 *mb* differ on the average by as much as 43 km. Epicenters from events with magnitudes 5.0–6.7  $M_w$  have a discrepancy of about 25 km on the average. The epicenters relocated using the SSST method of LIN and SHEARER (2005) correlate well with the bathymetry of the GoC and permit to infer the active transform faults. We found that the main events occur on or near transform faults and tend to have right-lateral strike slip focal mechanisms. Since epicenters located with regional stations have a much better azimuthal coverage and since we have accounted for 3D velocity variations by using source specific station term corrections, our results confirm, with a higher degree of confidence than previous studies, that the spatial distribution of seismicity is complex in the northern GoC whereas in

the southern GoC, it is confined to narrow zones near the most active faults.

### Acknowledgments

The operation of the RESBAN array (*Red Sismológica de Banda Ancha*) has been possible thanks to the financial support of the Mexican National Council for Science and Technology (CONACYT) by means of the projects 48852 and COC022. The NARS–Baja array was the result of a collaboration project among Utrecht University, California Institute of Technology and CICESE. The operation and data acquisition was possible thanks to Arie van Wettum, Robert Clayton, Jeannot Trampert and Hanneke Paulssen. Part of the analysis of this paper was made while one of the authors (RRC) was a UC MEXUS-CONACYT Visiting Scholar at the University of California, San Diego, IGPP-SIO. Peter Shearer kindly provided the modified version of the COMPLOC code. The useful comments and suggestions of the editor William Lee Bandy help us to improve the manuscript. We also thank the two anonymous reviewers.

### REFERENCES

- ARAGÓN-ARREOLA, M., and MARTÍN-BARAJAS, A. (2007), *Westward migration of extension in the Northern Gulf of California, Mexico*, Geology 35, 571–574
- CASTRO, R. R., SHEARER, P. M., ASTIZ, L., SUTER, M., JACQUES-AYALA, C., and VERNON, F. (2010), *The Long-lasting aftershock series of the 3 May 1887  $M_w$  7.5 Sonora Earthquake in the Mexican Basin and Range Province*, Bull Seism Soc Am 100, 1153–1164
- CLAYTON, R. W., TRAMPERT, J., REBOLLAR, C. J., RITSEMA, J., PER-SAUD, P., PAULSEN, H., PÉREZ-CAMPOS, X., VAN WETTUM, A., PÉREZ-VERTTI, A., and DI LUCCIO, F. (2004), *The NARS-Baja array in the Gulf of California Rift zone*, Margins Newslett 13, 1–4
- DEMETS, C. (1995), *A reappraisal of seafloor spreading lineations in the Gulf of California: implications for the transfer of Baja California to the Pacific Plate and estimates of Pacific-North America Motion*, Geophys Res Lett 22, 3545–3548
- EINSELE, G. (1982), *Mechanism of sill intrusion into soft sediment and expulsion of pore water*, Initial Rep Deep Sea Drill Proj 64, 1169–1176
- FABRIOL, H., DELGADO-ARGOTE, L.A., DANOBETIA, J.J., CÓRDOBA, D., GONZÁLEZ, A., GARCÍA-ABDESLEM, J., BARTOLOMÉ, R., and MARTÍN-ATIENZA, B. (1999), *Backscattering and geophysical features of volcanic rifts offshore Santa Rosalía, Baja California Sur, Gulf of California, México*, J Volcano Geotherm Res 93, 75–92

- GOFF, J.A., BERGMAN, E.A., and SOLOMON, S.C. (1987), *Earthquake source mechanism and transform fault tectonics in the Gulf of California*, J Geophys Res 92, 10485–10510
- GONZALEZ-FERNANDEZ, A., DAÑOBEITIA, J. J., DELGADO-ARGOTE, L. A., MICHAUD, F., CORDOBA D., and BARTOLOMÉ, R. (2005), *Mode of extension and rifting history of upper Tiburón and upper Delfín basins, Northern Gulf of California*, J Geophys Res 110, B01313. doi:[10.1029/2003JB002941](https://doi.org/10.1029/2003JB002941)
- ISACKS, B., OLIVER, J., and SYKES, L. (1968), *Seismology and the new global tectonics*, J Geophys Res 73, 5855–5899
- LIENERT, B. R. E., and HAVSKOV, J. (1995), *A computer program for locating earthquakes both locally and globally*, Seism Res Lett 66, 26–36
- LIN, G., and SHEARER, P. M. (2005), *Test of relative earthquake location techniques using synthetic data*, J Geophys Res 110, B04304. doi:[10.1029/2004JB003380](https://doi.org/10.1029/2004JB003380).
- LOMNITZ, C., MOOSER, F., ALLEN, C. R., BRUNE, J. N., and THATCHER, W. (1970), *Seismicity and tectonics of the Northern Gulf of California region, Mexico. Preliminary Results*, Geof Int 10, 37–48
- LONSDALE, P. L., *Geology and Tectonics History of the Gulf of California*, In: The Geology of North America: The Eastern Pacific Ocean and Hawaii (The Geological Society of America 1989).
- LÓPEZ-PINEDA, L., and REBOLLAR, C.J. (2005), *Source characteristics of the Mw 6.2 Loreto earthquake of 12 March 2003 that occurred in a transform fault in the middle of the Gulf of California, Mexico*, Bull Seism Soc Am 95, 419–430
- LÓPEZ-PINEDA, L., REBOLLAR, C. J., and QUINTANAR, L. (2007), *Crustal Thickness estimates for Baja California, Sonora, and Sinaloa, Mexico, using disperse surface waves*, J Geophys Res, 112, B04308. doi:[10.1029/2005JB003899](https://doi.org/10.1029/2005JB003899)
- MOLNAR, P. (1973), *Fault plane solutions of earthquakes and direction of motion in the Gulf of California and on the riveria fracture zone*, Geol Soc Am Bull 84, 1651–1658
- NAVA, F. A., and BRUNE, J. N. (1982), *An earthquake-explosion reversed refraction line in the peninsular ranges of southern California and Baja California Norte*, Bull Seism Soc Am 72, 1195–1206
- PACHECO, J. F., and SYKES, L. R. (1992), *Seismic moment catalog of large shallow earthquakes, 1900 to 1989*, Bull Seism Soc Am 82, 1306–1349
- PERSAUD, P., STOCK, J. M., STECKLER, M. S., MARTIN-BARAJAS, A., DIEBOLD, J. B., GONZALEZ-FERNANDEZ, A., and MOUNTAIN, G. S. (2003), *Active deformation and shallow structure of the Wagner, Consag, and Delfín basins, northern Gulf of California, Mexico*, J Geophys Res 108(B7), 2355. doi:[10.1029/2002JB001937](https://doi.org/10.1029/2002JB001937).
- PHILLIPS, R.P. (1964), *Seismic refraction Studies in the Gulf of California, in Marine Geology of the Gulf of California*, In Van Andel T. H., and Shor G.G., AAPG Mem 3, 90–121
- REBOLLAR, C. J., QUINTANAR, L., CASTRO, R. R., DAY, S. M., MADRID, J., BRUNE, J. N., ASTIZ, L., and VERNON, F. (2001), *Source characteristics of a 5.5 magnitude earthquake that occurred in the transform fault system of the Delfín basin in the Gulf of California*, Bull Seism Soc Am 91, 781–791
- REICHLE, M., and REID, I. (1977), *Detailed study of earthquake swarms from the Gulf of California*, Bull Seism Soc Am 67, 159–171
- REID, I., REICHLE, M., BRUNE, J., and BRADNER, H. (1973), *Micro-earthquake studies using sonobuoys, preliminary results from the Gulf of California*, J R Astronom Soc 34, 365–379
- RICHARDS-DINGER, K. and SHEARER P. (2000), *Earthquake locations in southern California obtained using source-specific station terms*, J Geophys Res, 105, 10939–10960
- RODRIGUEZ-LOZOYA, H. E., QUINTANAR, L., ORTEGA, R., REBOLLAR, C. J., and YAGI, Y. (2008), *Rupture process of four medium-size earthquakes that occurred in the gulf of California*, J Geophys Res, 113, B10301. doi:[10.1029/2007JB005323](https://doi.org/10.1029/2007JB005323).
- SYKES, L. R. (1968), *Seismological Evidence for Transform Faults, Sea-floor Spreading and Continental Drift*, in the History of the Earth's Crust, In (ed. Phinney), pp 120–150, Princeton Univ. Press, Princeton
- SYKES, L. R., (1970), *Focal mechanism solutions for earthquakes along the world rift system*, Bull Seismol Soc Am 60, 1749–1752
- THATCHER, W., and BRUNE, J. (1971), *Seismic study of an oceanic ridge earthquake swarm in the Gulf of California*, Geophys J R Astron Soc 22, 473–489
- TRAMPERT, J., PAULSEN, H., VAN WETTUM, A., RITSEMA, J., CLAYTON, R., CASTRO, R., REBOLLAR, C., and PÉREZ-VERTTI, A. (2003), *New array monitors seismic activity near the Gulf of California in México*, EOS, Trans Am Geoph Union 84, 29–32
- ZHANG, X., PAULSEN, H., LEBEDEV, S. and MEIER, T. (2007), *Surface Wave Tomography of the Gulf of California*, Geophys Res Lett, 34, L15305. doi:[10.1029/2007GL030631](https://doi.org/10.1029/2007GL030631)

(Received December 21, 2009, revised June 8, 2010, accepted June 16, 2010, Published online July 30, 2010)